

# We are IntechOpen, the world's leading publisher of Open Access books Built by scientists, for scientists

6,900

Open access books available

186,000

International authors and editors

200M

Downloads

Our authors are among the

154

Countries delivered to

TOP 1%

most cited scientists

12.2%

Contributors from top 500 universities



WEB OF SCIENCE™

Selection of our books indexed in the Book Citation Index  
in Web of Science™ Core Collection (BKCI)

Interested in publishing with us?  
Contact [book.department@intechopen.com](mailto:book.department@intechopen.com)

Numbers displayed above are based on latest data collected.  
For more information visit [www.intechopen.com](http://www.intechopen.com)



# Raman Spectroscopy in the Analysis of Textile Structures

*Dorota Puchowicz and Malgorzata Cieslak*

## Abstract

Raman spectroscopy as a non-destructive technique is very often used to analyze a historic or forensic material. It is also a very valuable method of testing textile materials, especially modified and functionalized. In the case of textiles, the advantages of this technique is the compatibility *inter alia* with FTIR, which is helpful in natural fibers identification or to distinguish between isomers and conformers of synthetic fibers. The work shows the possibility of special application of the Raman spectroscopy to the characterization of textile materials after modification and functionalization with nanoparticles. A functionalized textile structure with a metallic surface can provide a good basis for analytical studies using surface enhanced Raman spectroscopy as it was presented on the example of wool, cotton and aramid fibers.

**Keywords:** natural fibers, synthetic fibers, textile surface, functionalized textiles, SERS

## 1. Introduction

Raman spectroscopy is complementary method to FTIR Spectroscopy as both methods are based on detection of molecule vibrations. These spectroscopic techniques have different mechanism of vibrations detection and different physical phenomena are studied. Vibrations modifying the dipole moment of a molecule are active in IR spectroscopy, whereas vibrations modifying the polarizability of a molecule (i.e. stretching of C-C or C=C groups) are detected by Raman technique [1]. That is why Raman spectrum brings information about polymer backbone structure, conformation, orientation, crystallinity, density, etc. All this causes that Raman spectroscopy is a very useful tool in the analysis of polymers. As the intensity of Raman scattering does not depend directly on the volume of the tested sample application of the optical microscope together with the Raman spectrometer allows analysis of very small samples, including nanoparticles. Samples once studied in Raman spectrometer could be given for additional analysis by other techniques, if it is necessary. Therefore Raman spectroscopy is a valuable tool in analysis of ancient materials or forensic samples and also can be successfully applied in the textile materials study. Modern Raman spectrometers equipped with advanced software and volume mapping system allow the characterization of textile materials containing nanoparticles, their distribution on the surface of the material and inside the fiber analyzing its cross-section as well as in the case of colored materials, distribution of dyes, metal-dye interactions on the surface and inside the fiber structure [2–9]. The functionalization with metal nanoparticles and metal oxides plays now a special role, as it offers the possibility of giving textile products such

properties as: bioactivity, UV protection, catalytic or conductive properties [2–15]. Knowledge of the structure of the fibers, their physical, chemical properties as well as surface characteristics [2–5, 16–20] is extremely important in carrying out any modification. Application of nanoparticles is closely related to the use of advanced research methods necessary for the analysis of modified surfaces. Research on the fibrous structures modification using nanoparticles is the another area of analysis in which Raman spectroscopy can be successfully applied. Furthermore presence of noble metal nanoparticles on the fiber surface affects its Raman spectrum causing the effect of strengthening the Raman signal from the fiber itself and the contained substances (e.g. dye, modifier) [21–23]. Thus functionalized textile structure can be a good substrate for analytical studies using surface enhanced Raman spectroscopy.

## 2. Raman spectra of textile fibers

Raman spectroscopy, in general, is limited by fluorescence which often hides the Raman effect. However thanks to development of electronics and computing brought the possibility of Raman scattering enhancement, fluorescence minimalization, application different light sources in Raman spectrometers [24] significantly broadened analytical applications of this technique [25]. All Raman spectra presented in this chapter are performed on Raman Renishaw In via dispersive Spectrometer with Leica microscope. CCD detector of high quantum efficiency and extremely low intrinsic noise enabled to obtain Raman signal from textile substrate and 785 nm light excitation allowed overcome the fluorescence. Raman spectroscopy provides information about the structure of the fiber, e.g. the degree of crystallinity. Raman *inter alia* plays an important role in the analysis of hygroscopic fibers because, unlike FTIR, water does not affect the spectrum and is very useful in analysis of organic systems with C-C or C=C bonding.

### 2.1 Natural fibers

Cotton is the most commonly used natural plant fiber and the second most popular fiber, next to polyester [26]. The main component of the cotton fiber is cellulose over 88%, other component pectin, wax, proteins and other organic materials do not exceed 2% [27]. In Raman spectrum (**Figure 1**) the most intense bands are the stretching vibrations of symmetric and asymmetric COC glycosidic ring breathing, skeletal stretching; at  $1099\text{ cm}^{-1}$  asymmetric and  $1125\text{ cm}^{-1}$  symmetric. Another vibrations characteristic for cotton are at:  $331$  and  $381\text{ cm}^{-1}$  of CCC ring deformations bending, at  $438$  and  $460\text{ cm}^{-1}$  of CCC, CCO ring deformation and skeletal bending, at  $520\text{ cm}^{-1}$  COC glycoside linkage and CCC ring deformation bending, at  $901, 1001\text{ cm}^{-1}$  HCC, HCO skeletal rotating. Stretching vibrations of CC and CO of glycosidic ring are at  $1156\text{ cm}^{-1}$ . Cluster of bands in the region between  $1200$  and  $1500\text{ cm}^{-1}$  concerns the  $\text{CH}_2$  twisting at  $1297\text{ cm}^{-1}$ ,  $\text{CH}_2$  wagging  $1341\text{ cm}^{-1}$ ,  $\text{CH}_2$  bending at  $1384\text{ cm}^{-1}$ ,  $\text{CH}_2$  bending scissors at  $1484\text{ cm}^{-1}$  [28, 29]. In this cluster should be also bending vibrations of alcohol COH that are overlapped. In the spectrum there are also present stretching bands of CH vibrations at  $2903\text{ cm}^{-1}$ .

Wool and silk are animal protein fibers [30]. Wool consists mainly of keratin which is sulfur possessing protein. Silk consists mainly of fibroin protein. In analysis of wool and silk, by vibrational spectroscopy techniques, Raman spectroscopy is the method that allows for their unambiguous identification. IR Spectra of wool and silk are very similar (**Figure 2**). No significant differences, even in fingerprint region could be observed, even differences in relative peak intensities or wavenumber shifts are very subtle. Only the band shapes in the area over  $2900\text{ cm}^{-1}$

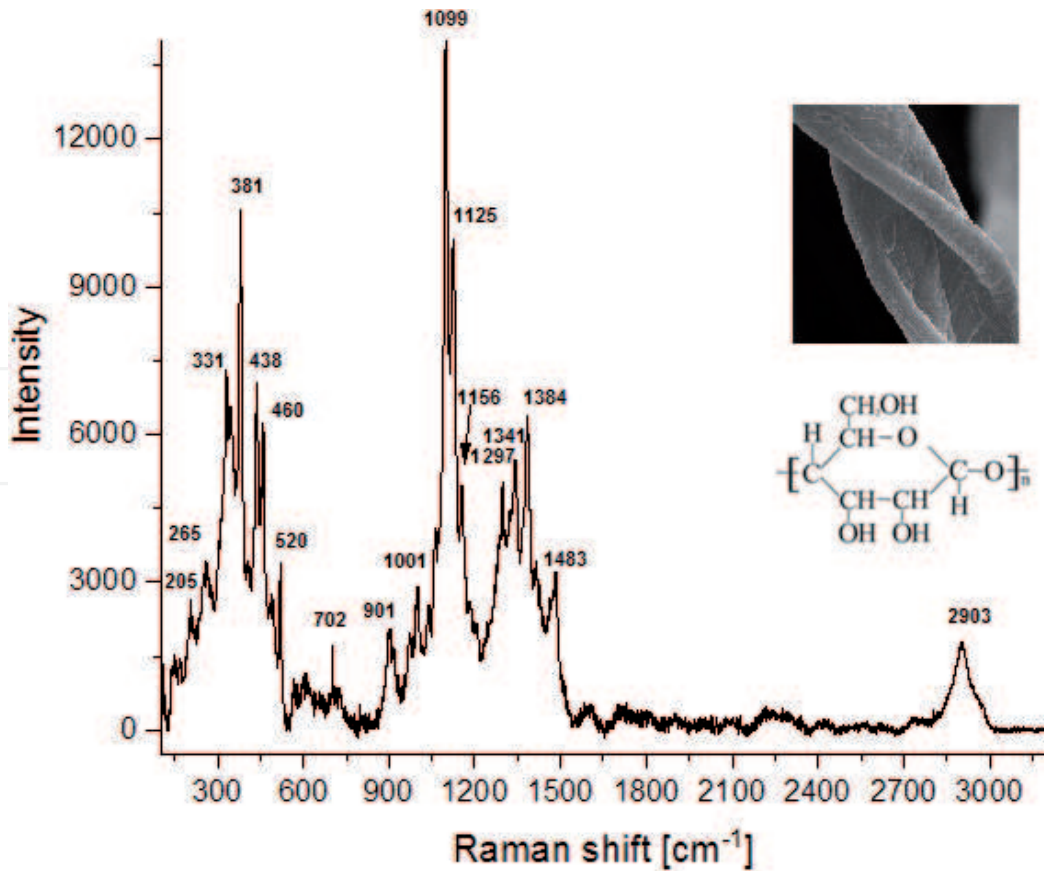


Figure 1.  
 Raman spectrum of cotton fiber.

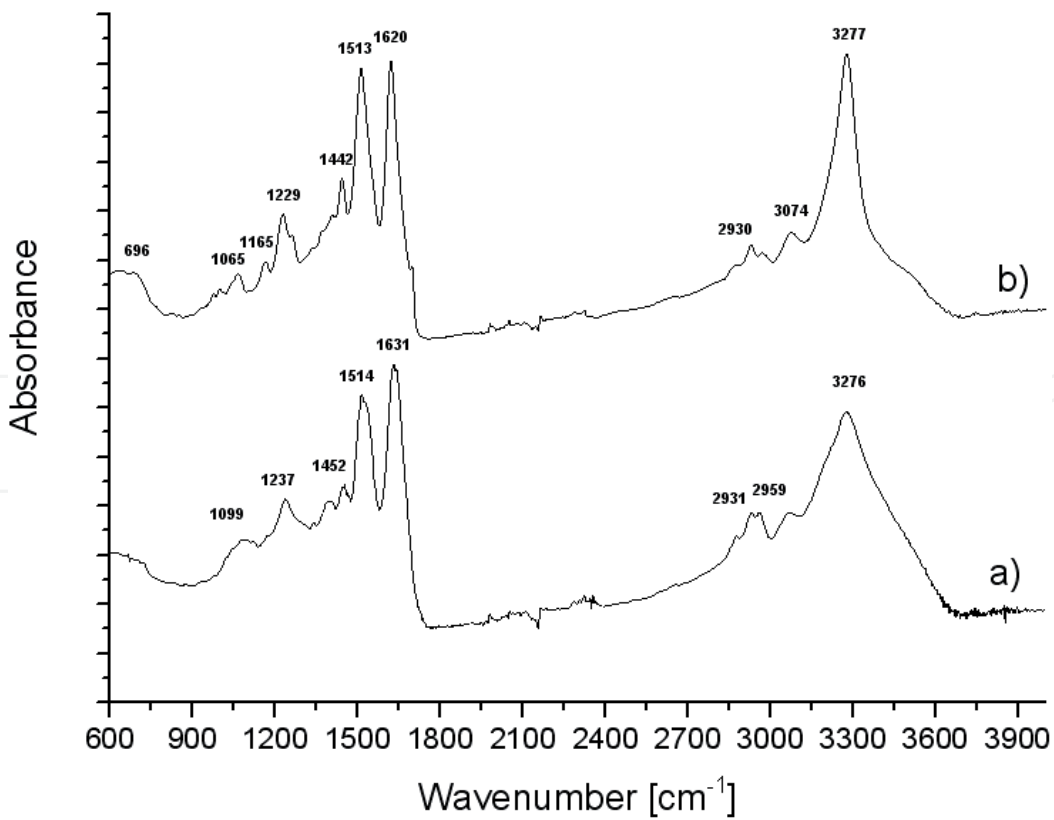
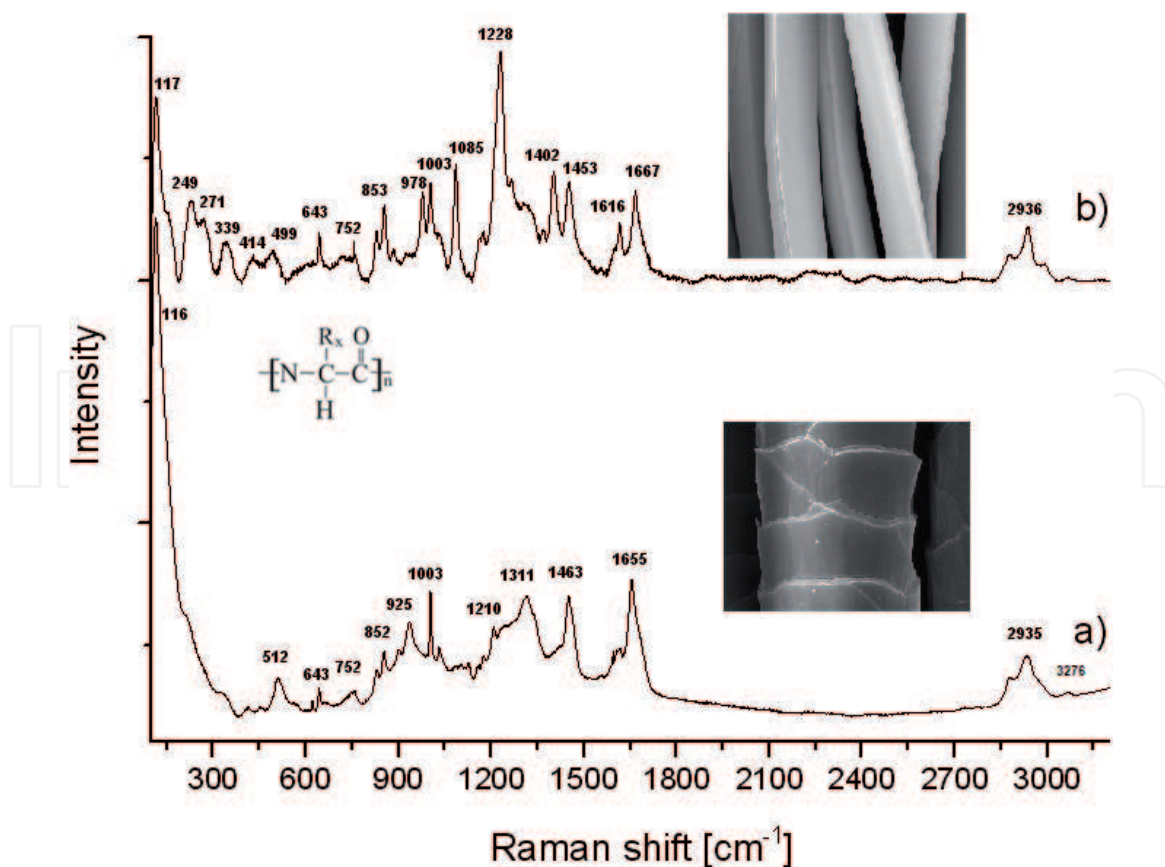


Figure 2.  
 IR spectrum of: a) wool, b) silk.

distinguishes these fibers. However these slight differences are visible when the wool and silk spectra are aligned as it is shown in **Figure 2a** and **b**. Therefore, the use for the fiber identification the complementary method is recommended.



**Figure 3.**  
Raman spectrum of: a) wool, b) silk.

The Raman measurement on wool and silk will help to distinguish between the two protein fibers, as the spectra obtained are clearly different (**Figure 3a** and **b**). This is possible thanks to the sensitivity of this technique to differences in the organic structures, in this case the sequence of amino acids [30]. Silk fibroin is the protein mainly consists of alanine (44,1%) and glycine (26,5%). There are also present in smaller amounts serine (11,8%), tyrosine (4,9%), aspartic acid (4,7%) and arginine (2,6%). The content of other amino acids does not exceed 1%, and, at the same time there is no cysteine, that is one the basic components of wool keratin. Wool keratin in the protein that mainly consists of glutamic acid (11,9%), serine (10,4%), cysteine (10,3%), glycine (8,4%), leucine (7,7%), arginine (6,9%), proline (6,6%) and other amino acids [31]. The different sequence of amino acids directly translates into different Raman characteristics and the fingerprint of wool and silk differ substantially. The most important observed feature in Raman spectrum of wool is the presence of band at  $512\text{ cm}^{-1}$  characteristic to S-S disulphide bridge coming from cysteine [31, 32].

While in case of silk there is sequence of amino acids skeletal vibrations in the region of  $100\text{--}500\text{ cm}^{-1}$  and the dominating band of amide  $\text{CH}_2$  bending at  $1228\text{ cm}^{-1}$  [33]. The more detailed description of wool and silk Raman characteristic bands is listed in **Table 1**.

## 2.2 Synthetic fibers

Today most textile products are made of synthetic fibers (approx. 62%) [26], therefore they are the subject of research, including functionalization. Over the 50% of all fibers on the world market are polyester fibers (PET) Another popular synthetic fibers are nylon, acrylic, polypropylene, aromatic polyamides: meta- and para-aramid. Aramid fibers due to their properties, such flame retardance, mechanical or thermal resistance are the class of heat resistant, flame retardant and

Wool [21]		Silk [23]	
Raman shift [cm <sup>-1</sup> ]	Description	Raman shift [cm <sup>-1</sup> ]	Description
512	SS stretching	117,249, 271, 339, 414, 499	CCC def CCN, combinations of backbone deformations with pendant chains
643	CS stretching	643	NCH bending Amid IV
752	CCC, stretching	752	CH <sub>2</sub> CH <sub>3</sub> skeletal alanine
852	CH <sub>2</sub> , HCS bending, CCOO <sup>-</sup> stretching	853	CC skeletal tyrosine
		978	CH <sub>2</sub>
925	C-C skeletal bending	1003	CH <sub>2</sub> bending
1003	NCH bending	1085	CC skeletal
1210	NH deformation, C-N elonging	1228	CH <sub>2</sub> bending Amid III
1311,1463	CH <sub>2</sub> bending, COO <sup>-</sup> bending	1402	CH <sub>2</sub> bend
1514, 1631	CH, NH bending	1453	CH <sub>2</sub> bending scissors
1665	C=O, COO <sup>-</sup> stretching (Amide I)	1616	C=C stretching (Tyrosine)
2931, 2959	CH stretching	1667	Amide I
		2935	CH stretching

**Table 1.**  
 Raman characteristic bands of wool and silk.

strong synthetic fibers. They are important in military applications i.e. for firefighters clothing or bullet resistant vests [34]. In the case of synthetic polymers, it is also important, that the intensity of Raman scattering is stronger than fluorescence. Raman spectra of Polyester (PET), nylon fibers (Polyamide 6 (PA 6) and Polyamide (6.6 PA 6.6), polypropylene (PP), polyacrylic fiber (PAN), meta-aramid (mAr) and para-aramid (pAr) are presented below and discussed.

In Raman spectrum of polyethylene terephthalate (PET) fiber [35–37] there are two dominating very intense bands: at 1615 cm<sup>-1</sup> that is C-C aromatic ring and at 1728 cm<sup>-1</sup> – carbonyl C=O stretching. Another characteristic bands of PET are: 278 cm<sup>-1</sup> deformation skeletal C-C, 702 cm<sup>-1</sup> ring C-C stretch, 859 cm<sup>-1</sup> C-C, COC bending, 998 cm<sup>-1</sup>, 1096 cm<sup>-1</sup> C-O and C-C stretch, 1181 cm<sup>-1</sup> C-C ring stretch, 1289 cm<sup>-1</sup> CO-O stretch, 1416, 1463 cm<sup>-1</sup> CH<sub>2</sub> bending. Band at 142 cm<sup>-1</sup> belongs to TiO<sub>2</sub> which is often used in the processing of the fiber, as a matting agent.

Raman spectrum of PET gives information about the polymer form. Textile polymers are not 100% crystalline, they also have amorphous areas, therefore the degree of crystallinity is determined for them. In the crystalline state the ethylene glycol units of PET have a *trans* structure while the amorphous state PET has a *gauche* structure of the ethylene glycol units [35]. An intense peak at 1,096 cm<sup>-1</sup> indicates that analyzed PET fiber is in crystalline form. However, the carbonyl band at 1728 cm<sup>-1</sup> is considered a better marker of crystallinity [35]. The highly crystalline samples give a narrow carbonyl peak; whereas for the amorphous the band width is demonstrably broader. In presented spectrum (**Figure 4**) peak at 1728 cm<sup>-1</sup> is narrow, so the crystalline form is confirmed.

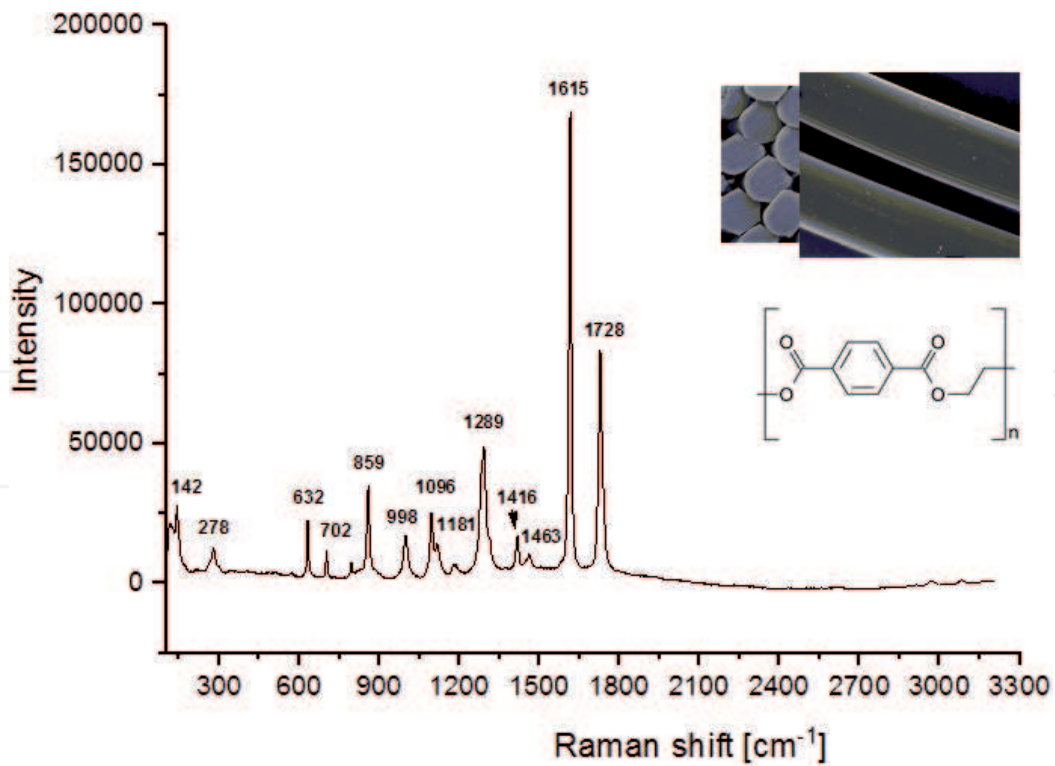


Figure 4.  
Raman spectrum of PET fiber.

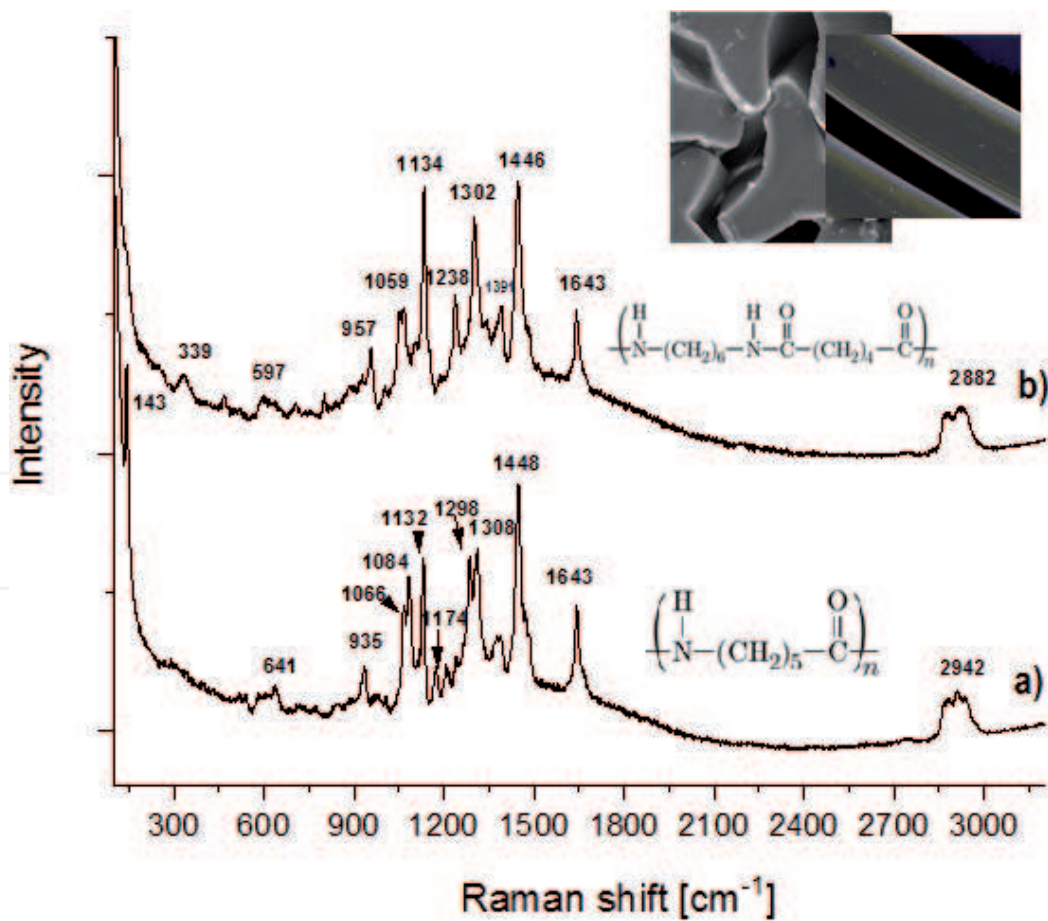


Figure 5.  
Raman spectrum of polyamide fibers: a) PA 6, b) PA6.6.

Polyamides are polymers in which an amide group  $-NH-CO-$  joins the monomer units. Two most important commercially textile polyamides are Polyamide 6 (PA 6) and Polyamide 6.6 (PA 6.6). In both polyamides the monomeric units contains six

carbon atoms. They can be distinguished most easily by examining the melting point. However, these analysis requires destruction of the sample. Raman spectroscopy is in this case very good method for polyamide type identification, used in practice i.e. in the carpet recycling [38]. Raman Spectrum of PA 6 (**Figure 5a**) shows CC deformation at  $643\text{ cm}^{-1}$ , CCO stretching at  $935\text{ cm}^{-1}$ , CC skeletal stretching at  $1066, 1084$  and  $1132\text{ cm}^{-1}$ , CN stretching and NH bending of amide III at  $1298\text{ cm}^{-1}$ ,  $\text{CH}_2$  twisting at  $1308\text{ cm}^{-1}$ ,  $\text{CH}_2$  bending at  $1448\text{ cm}^{-1}$ ,  $1643\text{ cm}^{-1}$  C=O stretching and CH stretching at  $2942\text{ cm}^{-1}$  [39].

There is also present band at  $143\text{ cm}^{-1}$  of  $\text{TiO}_2$  used in fiber processing. While in the Raman spectrum polyamide 6.6 (**Figure 5b**) CC deformation at  $643\text{ cm}^{-1}$ , CCO stretching at  $957\text{ cm}^{-1}$ , CC skeletal stretching at  $1059$  and  $1134\text{ cm}^{-1}$ , NH deformation at  $1238\text{ cm}^{-1}$ , twisting at  $1302\text{ cm}^{-1}$ ,  $\text{CH}_2$  bending at  $1446\text{ cm}^{-1}$ ,  $1643\text{ cm}^{-1}$  C=O stretching and CH stretching at  $2882\text{ cm}^{-1}$  are present [39]. The Raman spectra of both polyamides differ from each other the presence of three skeletal CC bands ( $1066, 1084$  and  $1132\text{ cm}^{-1}$ ) in the case of PA 6 and two CC skeletal bands ( $1059$  and  $1134\text{ cm}^{-1}$ ) in the case of PA 6.6. Moreover PA 6,6 spectrum does not have an amide III band (C–N stretching and N–H bending) at  $1298\text{ cm}^{-1}$ , which is present in PA 6 spectrum.

Polypropylene fibers are the most commercially important polyolefin fibers, whose polymer chain consists of olefin units. Raman spectrum of PP (**Figure 6**) contains:  $\text{CH}_2\text{-CH-CH}_3$  torsions in the polymer backbone at  $107$  and  $175\text{ cm}^{-1}$  [40],  $\text{CH}_2$  wagging and CH bending at  $251$  and  $399\text{ cm}^{-1}$ ,  $\text{CH}_2$  wagging and CH bending at  $320$  and  $455\text{ cm}^{-1}$ ,  $\text{CH}_2$  wagging,  $\text{CH}_2$  bending and  $\text{CCH}_3$  stretching at  $528\text{ cm}^{-1}$ , CC backbone stretching,  $\text{CH}_2$  wagging,  $\text{CCH}_3$  stretching at  $809\text{ cm}^{-1}$ , CC backbone stretching,  $\text{CH}_2$  wagging,  $\text{CCH}_3$  stretching,  $\text{CH}_3$  bending at  $847\text{ cm}^{-1}$ , CC backbone stretching,  $\text{CH}_3$  rocking at  $947\text{ cm}^{-1}$ ,  $\text{CH}_3$  rocking,  $\text{CH}_2$  wagging, CH bending at  $999\text{ cm}^{-1}$ , CC backbone stretching,  $\text{CCH}_3$  stretching, CH bending at  $1038\text{ cm}^{-1}$ , CC backbone stretching,  $\text{CCH}_3$  stretching, CH bending and  $\text{CH}_3$  bending at  $1153\text{ cm}^{-1}$ ,

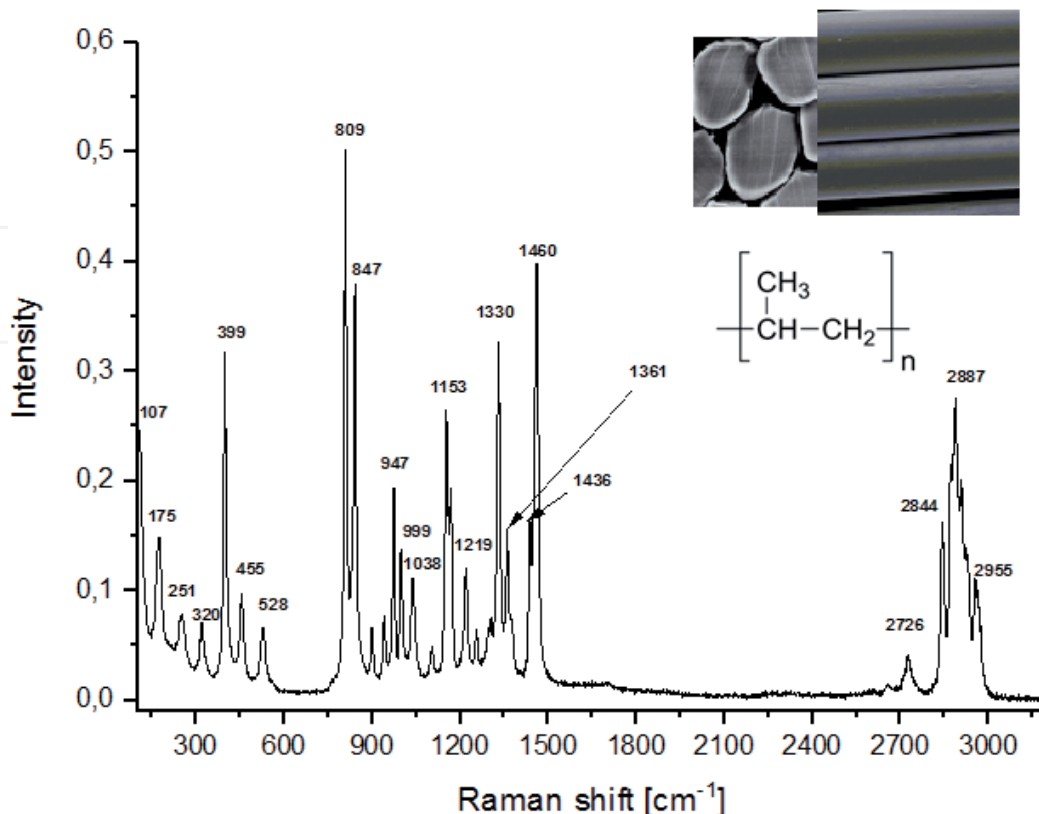


**Figure 6.**  
Raman spectrum of PP fiber.

CC backbone stretching, CH bending and CH<sub>2</sub> twisting at 1219 cm<sup>-1</sup>, CH bending, CH<sub>3</sub> symmetric bending at 1361 cm<sup>-1</sup>, CH<sub>3</sub> asymmetric bending at 1436 cm<sup>-1</sup>, CH<sub>3</sub> asymmetric bending and CH<sub>2</sub> bending at 1460 cm<sup>-1</sup>, symmetric CH<sub>2</sub> stretching at 2726 cm<sup>-1</sup>, symmetric CH<sub>3</sub> stretching at 2844 cm<sup>-1</sup> and 2887 cm<sup>-1</sup>, asymmetric CH<sub>3</sub> stretching and 2955 cm<sup>-1</sup> [41].

The skeleton C-C vibrations of PP are sensitive to conformation effects, thus the vibrations at 809 cm<sup>-1</sup> and 842 cm<sup>-1</sup> are connected to crystallinity of PP. The band at 809 cm<sup>-1</sup> corresponded to vibrations of the crystalline moieties, whereas the band at 842 cm<sup>-1</sup> to non-crystalline part [42].

Polyacrylic fibers used in the manufacturing of textiles are composed of at least 85% by weight of polyacrylonitrile and 4–10% of non-ionic comonomer and 0,5–1% of an ionic co-monomer [43]. This is due that fibers produced from 100% polyacrylonitrile have poor elasticity and they are difficult to dye [44]. Polyacrylonitrile (PAN) is produced by the polymerization of cyanoethene and nitrile CN group is the characteristic element of this polymer. In IR spectroscopy is the very useful method in the subclasses of acrylic distinguishing the additional comonomers and additives [39]. In Raman spectrum mostly polyacrylic polymer is visible. Presence of another monomers is not evident in Raman spectrum, they show only minor variations in band shapes [39].

In the Raman spectrum of PAN fiber (**Figure 7**) the dominant band is the nitrile CN stretching band at 2245 cm<sup>-1</sup>. Another characteristic bands of PAN concern the CH<sub>2</sub> bending at 1455 cm<sup>-1</sup>, CH bending at 1314 cm<sup>-1</sup>, CN twisting at 1225 cm<sup>-1</sup>, CC skeletal stretching at 1118 and 1102 cm<sup>-1</sup>, CH<sub>2</sub> twisting and CCN stretching at 829 cm<sup>-1</sup>, CN wagging and bending 638 cm<sup>-1</sup>, CN bending at 516 cm<sup>-1</sup>, CC backbone deformation at 397 cm<sup>-1</sup> and 283 cm<sup>-1</sup>. Band at 142 cm<sup>-1</sup> belongs to TiO<sub>2</sub> used in fiber processing. Weak carbonyl band at 1737 cm<sup>-1</sup> belongs to vinyl acetate monomer [39].

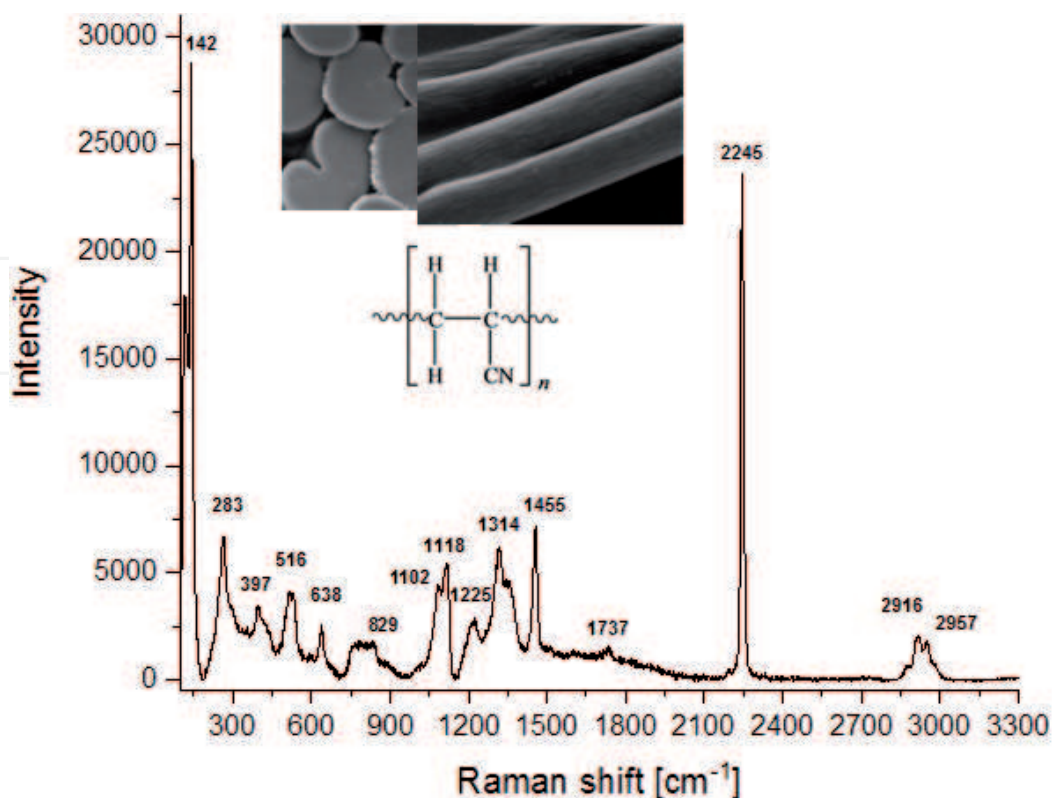


**Figure 7.**  
Raman spectrum of PAN fiber.

Aramid fibers are made from aromatic polyamide polymers. Aramid chains possess amide groups which are directly connected to two aromatic rings: meta aramid (mAr) contains m-disubstituted benzene rings, para aramid (pAr) contains p-disubstituted benzene rings. Raman spectra of aramid fibers (**Figure 8**) are presented in the range  $100\text{--}2000\text{ cm}^{-1}$  for better readability, as no bands were recorded in the  $2000\text{--}3000\text{ cm}^{-1}$  area. Lack of the bands in the  $2900\text{--}3200\text{ cm}^{-1}$  region characteristic of CH and NH stretching vibrations was interpreted to be due an orientational effects [45]. In the spectra of meta aramid (**Figure 8a**) characteristic Raman bands occur at  $115\text{ cm}^{-1}$  (CC in-plane bending), at  $192\text{ cm}^{-1}$  (ring out of plate CCC bending vibration), at  $278\text{ cm}^{-1}$  (ring CCC asymmetric deformation, CN in-plane bending), at  $659\text{ cm}^{-1}$  (ring puckering deformation, ring bending and asymmetric torsion, CH out-of-plane deformation), at  $1003\text{ cm}^{-1}$  (trigonal ring breathing vibration CH in plane bending, ring and ring CH deformation), at  $1250\text{ cm}^{-1}$  (NH bending and CN stretching),  $1339\text{ cm}^{-1}$  (CH in-plane deformation), at  $1420$  and  $1442\text{ cm}^{-1}$  (ring puckering vibration, aromatic CH bending),  $1488\text{ cm}^{-1}$  (CH in-plane and NH in-plane bending), at  $1547\text{ cm}^{-1}$  (NH in-plane bending), at  $1606\text{ cm}^{-1}$  (CC aromatic ring stretching), at  $1655\text{ cm}^{-1}$  (amide stretch C=O). In the spectrum of pAr (**Figure 8b**) characteristic Raman bands occur at  $154\text{ cm}^{-1}$ , at  $633\text{ cm}^{-1}$  (CC ring in plane deformation), at  $698\text{ cm}^{-1}$  (CH out-of-plane deformation; CO bending), at  $739\text{ cm}^{-1}$  (CO in-plane bending; ring asymmetric CH deformation; CN stretching), at  $789\text{ cm}^{-1}$  (CH out-of-plane deformation, CCC ring puckering deformation), at  $845\text{ cm}^{-1}$  (CH out-of-plane deformation; ring CC stretching, ring bending and asymmetric torsion), at  $919\text{ cm}^{-1}$  (ring out-of-plane bending, CH in-plane bending, CH in-plane ring bending mode, CC stretching),  $1186\text{ cm}^{-1}$  (ring CH deformation), at  $1280\text{ cm}^{-1}$  (NH bending and CN stretching, CC stretching), at  $1332\text{ cm}^{-1}$  (ring CH bending, ring CC stretching), at  $1414\text{ cm}^{-1}$  (symmetric ring puckering/aromatic CH in-plane), at  $1520\text{ cm}^{-1}$  (ring CH bending), at  $1576\text{ cm}^{-1}$  (amide II vibration, bend (NH) and stretch (CN), ring CC stretching; NH bending), at  $1615\text{ cm}^{-1}$  (aromatic ring CC stretching),  $1652\text{ cm}^{-1}$  amide I (CO stretching) [45].

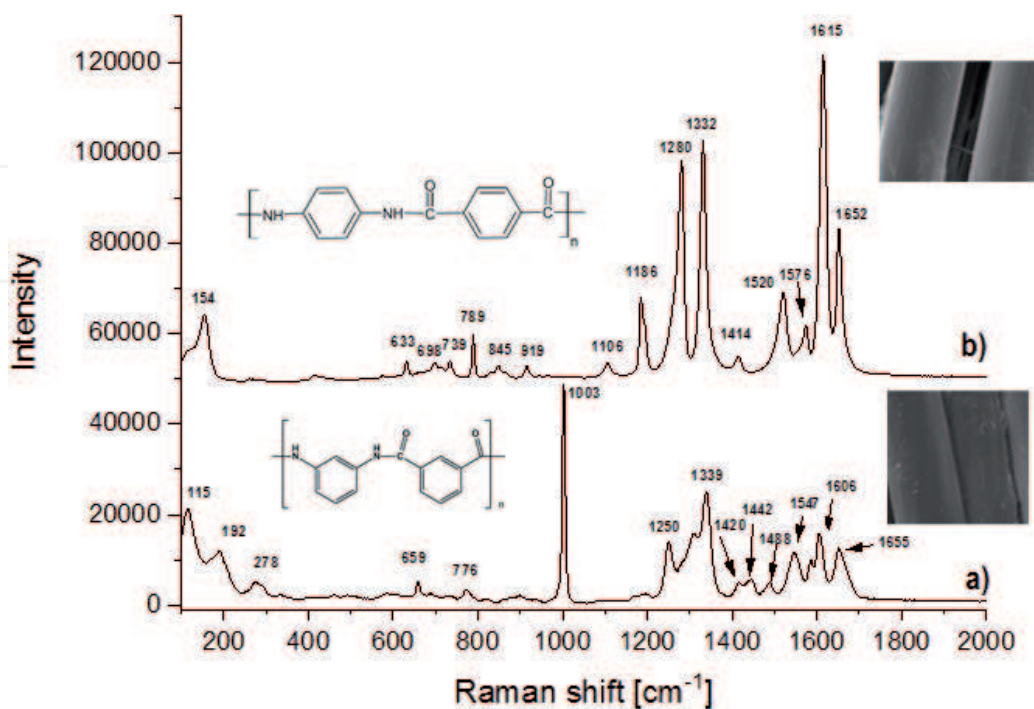


**Figure 8.**  
Raman spectrum of aramid fibers: a) mAr, b) pAr.

Thus mAr could be identified by three characteristic Raman bands concerning CCC ring bending vibrations (at 115, 192 and 278  $\text{cm}^{-1}$ ), and the presence intense band of ring breathing vibration (at 1003  $\text{cm}^{-1}$ ). Spectrum of pAr exhibits characteristic Raman bands associated with p-substituted benzenes and may be identified by strong band at 154  $\text{cm}^{-1}$  (unassigned), ring deformation bands at 789  $\text{cm}^{-1}$  and 1182  $\text{cm}^{-1}$ , NH bending and CN stretching band at 1280  $\text{cm}^{-1}$ , ring CH bending and CC stretching at 1332  $\text{cm}^{-1}$  and the intense band of aromatic ring CC stretching at 1615  $\text{cm}^{-1}$ . The Raman spectroscopy is a very good method for nondestructive and unambiguous identification of the aramid fibers as the spectra of mAr are sufficiently different from those of the pAr to enable a definitive distinguishing.

### 3. Textile modified structures

Growing market demand for functional textile materials has followed the development of research on the fibrous structures modification using nanoparticles [2–23]. Modern multi-functional textiles are based very often on fibers surface modified with nanoparticles. The most extensively studied nanomaterial for textile modification is nanosilver. Over 200 publications a year concerning the textile functionalization by nanosilver appeared between 2015 and 2020 [46]. The second most studied nanoscale material, just behind silver is TiO<sub>2</sub> with more than 100 publications per year since 2011 [46].

#### 3.1 Characterization of functional textiles with silver nanowires (AgNWs)

Application of silver nanowires AgNWs for textile functionalization allows for obtaining bifunctional textiles with bioactive and conductive properties [4–5]. AgNWs colloid of 0,5% concentration was synthesized [4, 44, 46, 47] and nanowires were applied to the surface of the fabrics by dipping and drying method [4–5].

Raman rectangle map of functionalized cotton is presented on **Figure 9**. Characterization of cotton modified by AgNWs was described in publications [4, 12].

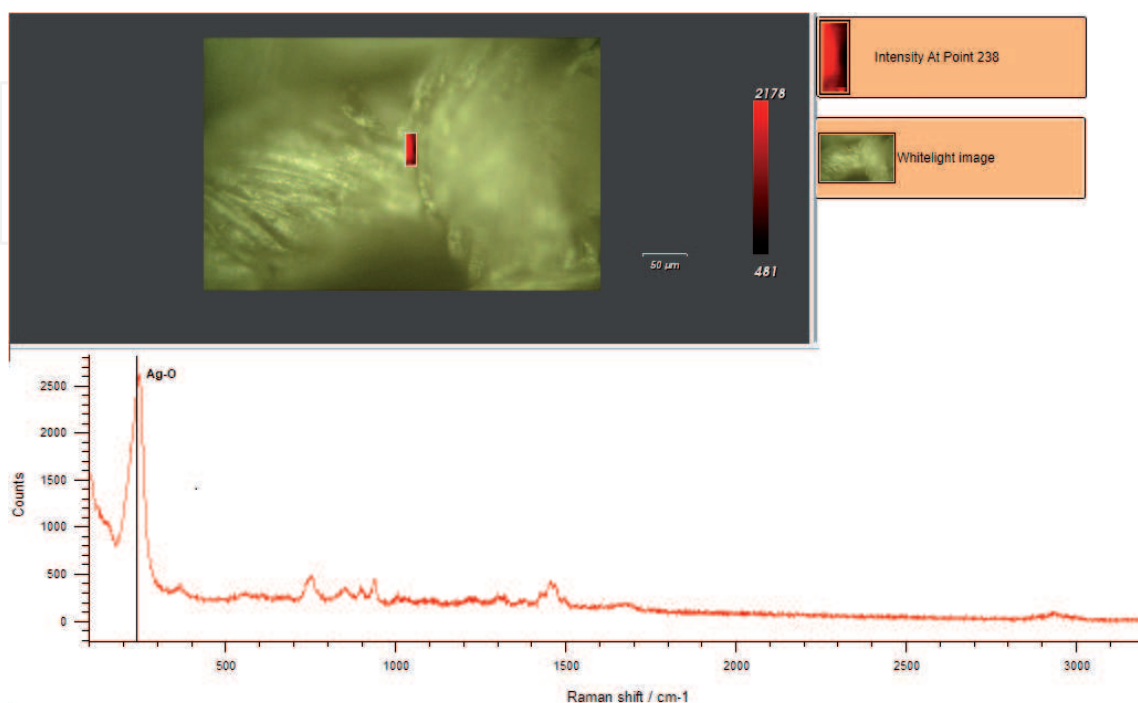


**Figure 9.**  
Raman map of cotton fabric functionalized by AgNWs.

Raman technique thanks to Raman mapping enables the characterization of the selected surface area on a micro scale. The analyzed area is visualized in terms of the intensity of the band characteristic for a given material or modifier. Two or even three dimensional maps (2D and 3D maps) show the distribution of the modifier on the analyzed area. Band characteristic for AgNWs is in the region  $240\text{--}250\text{ cm}^{-1}$  and it is the result of Ag-O coordination band that is the effect of interactions between silver and oxygen adsorbed on the surface [4, 22, 48]. In the case of modified cotton AgNWs, no cotton bands are visible on the surface. All analyzed surface is covered with a metallic AgNWs coating. The map was made according to the characteristic band of Ag-O coordination at  $238\text{ cm}^{-1}$ .

Characterization of functionalized aramid fibers is presented on **Figures 10** and **11**. For the functionalized mAr, the most intense band of mAr is the ring breathing band at  $1003\text{ cm}^{-1}$ . Raman maps were performed according to the  $1003\text{ cm}^{-1}$  band and according to AgNWs band which is represented by Ag-O coordination band at  $238\text{ cm}^{-1}$  (**Figure 10**). Both maps are also presented in 3D form.

Whereas for the functionalized pAr, the characteristic band of mAr was the NH bending and CN stretching band at  $1279\text{ cm}^{-1}$ , characteristic band of AgNWs was Ag-O coordination band (**Figure 11**). In both figures (**Figures 10** and **11**), the blue color shows the area covered with nanowires, and the red color indicates that aramid predominates on the surface in the studied area.

### 3.2 Characterization functional textiles with $\text{TiO}_2$ on the surface

Titanium dioxide ( $\text{TiO}_2$ ) applied to the modification of textile materials can give them such properties as i.e. photocatalytic, self-cleaning, bioactive, UV protective etc. [2, 9, 49–52]. Raman map of  $\text{TiO}_2$  modified PP is presented on **Figure 12**.

Polypropylene as a one of the most used component of floorcoverings was also modified by  $\text{TiO}_2$ . Titanium dioxide was applied to limit the environmental tobacco

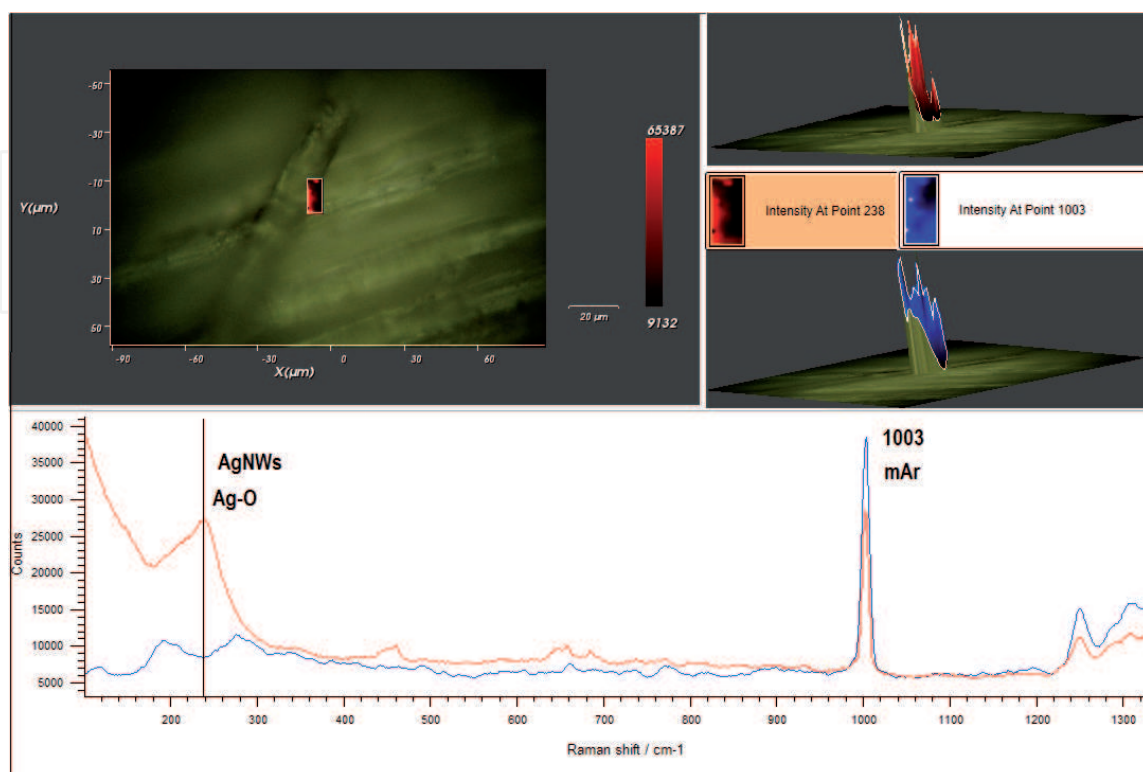


**Figure 10.**  
Raman map of mAr modified by AgNWs.

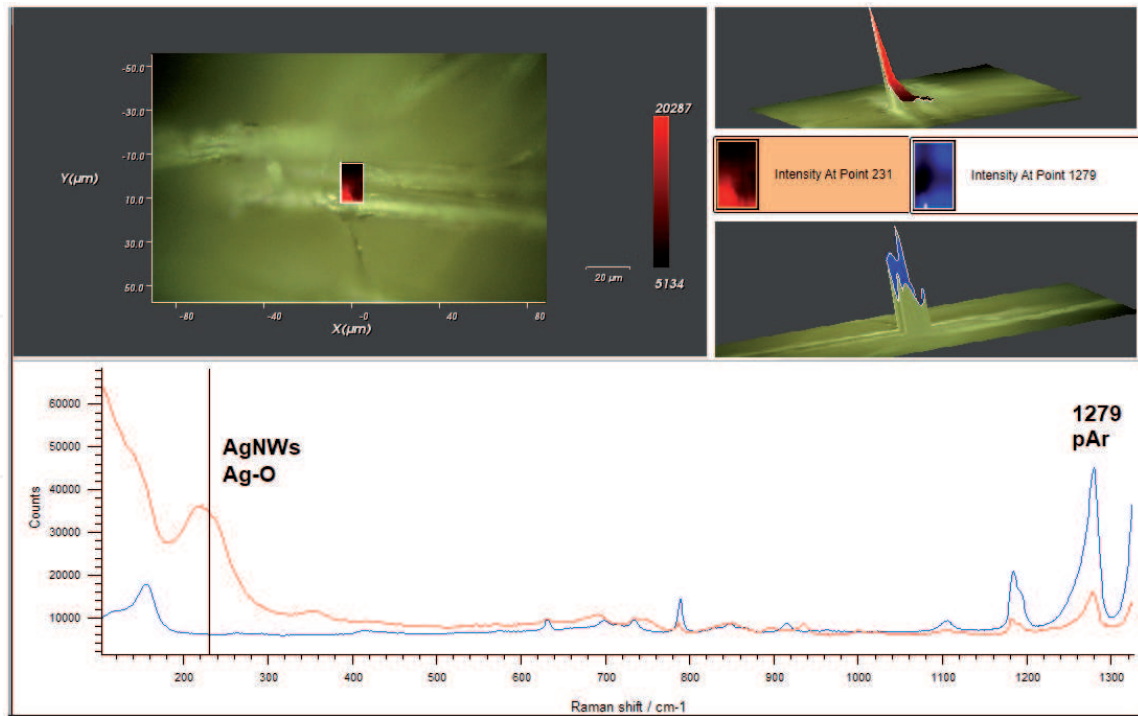


**Figure 11.**  
Raman map of pAr modified by AgNWs.

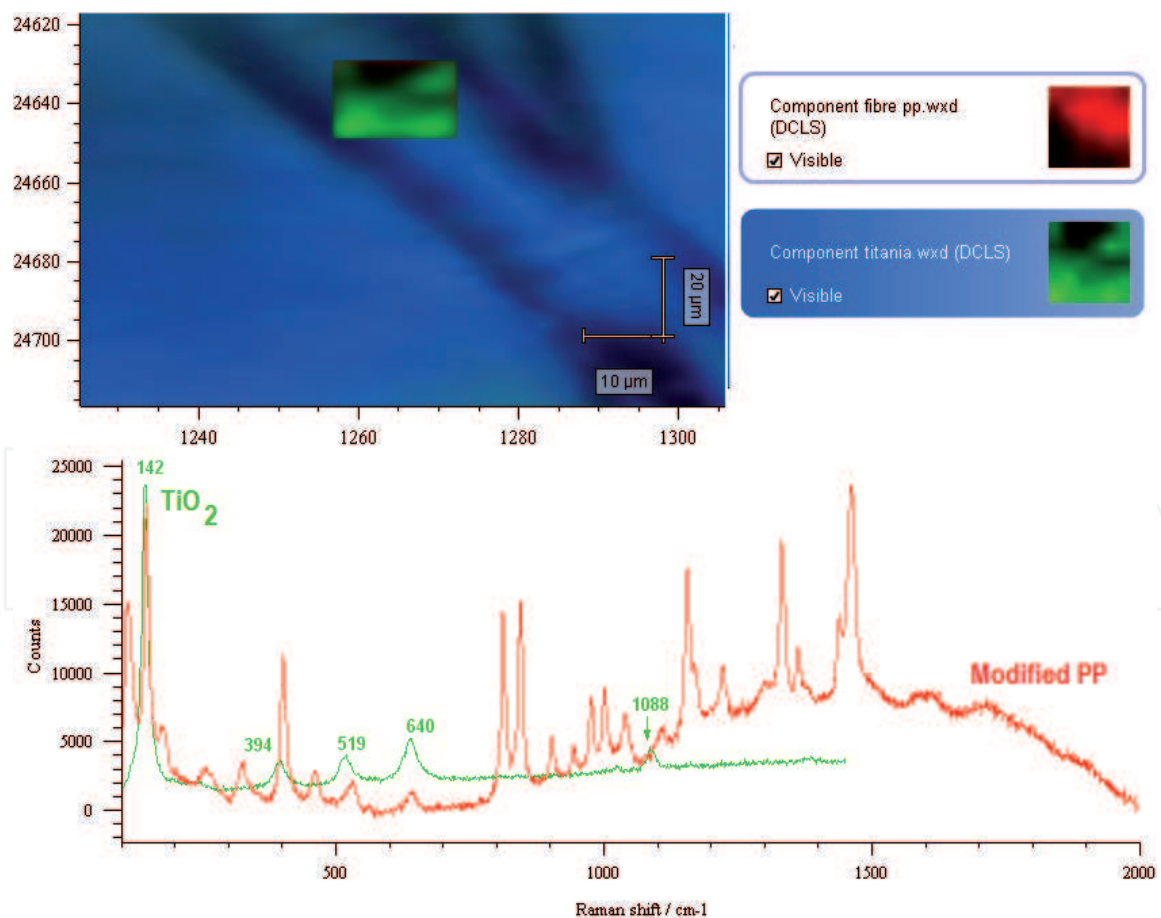


**Figure 12.**  
Raman map of PP fiber modified by  $\text{TiO}_2$ .

smoke (ETS) sorption by the photocatalytic decomposition of ETS-derived nicotine (basic marker of tobacco smoke exposure) [50–52]. Thanks to Raman Surface mapping the  $\text{TiO}_2$  distribution on the PP fiber can be evaluated. The analyzed area

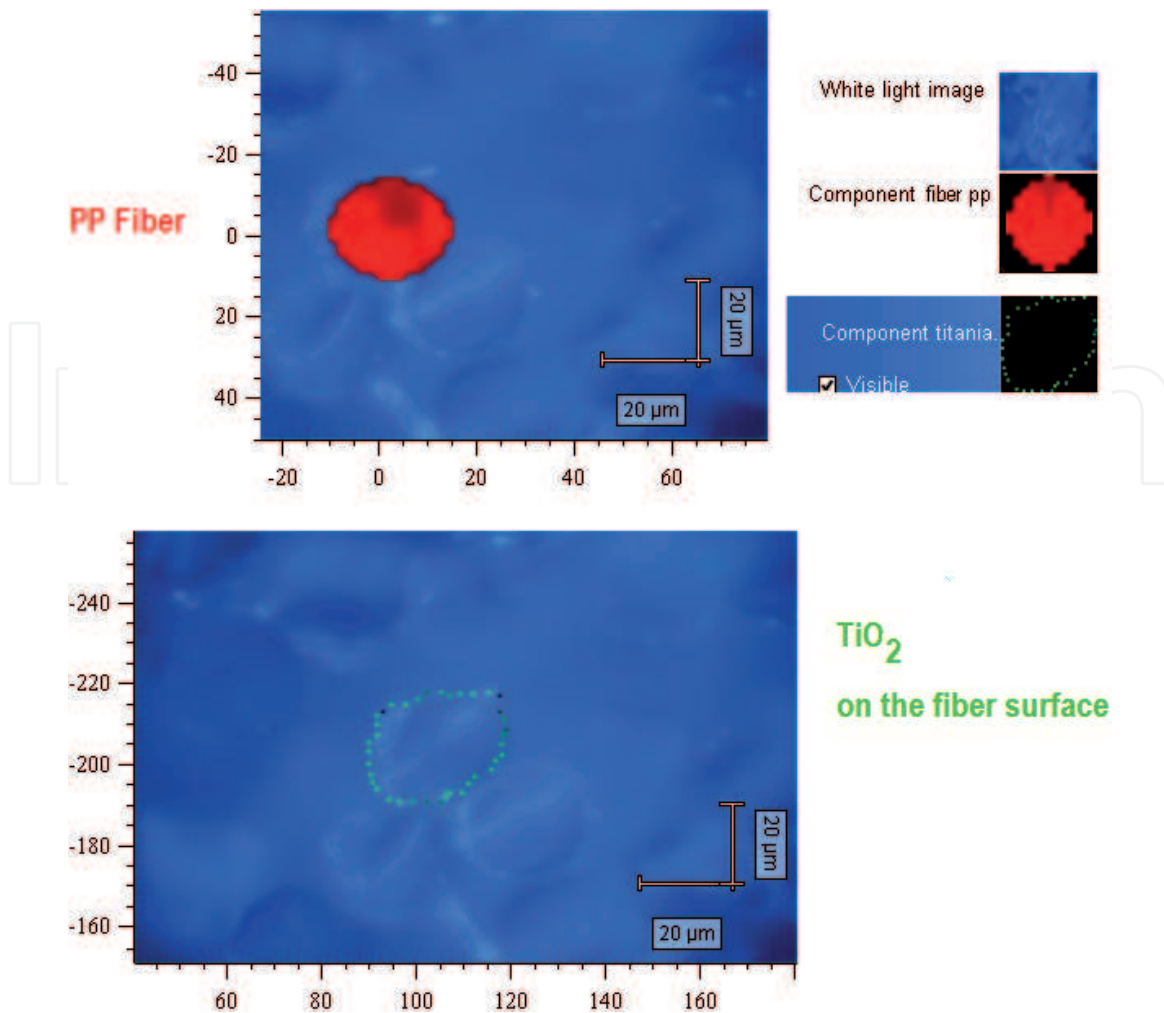


**Figure 13.**  
*Cross-sections of PP fibers modified with TiO<sub>2</sub>.*

is visualized in terms of the intensity of the  $142\text{ cm}^{-1}$  band that is characteristic for TiO<sub>2</sub> in anatase form [52]. The characteristics of functional fiber can be enriched by the cross-section map as it is shown on the **Figure 13**. The cross-section map illustrates the place of modification revealing whether the modification takes place on the surface, or in the volume of the fiber.

#### 4. SERS effect on textile fibers surface

The functionalization of textile with silver nanoparticles causes formation of metallic layer on their surfaces and in consequence possibility of Raman signal enhancement [4, 21–23]. The research on the functionalization of fibers has shown that a textile material can be a good carrier for the SERS effect [22]. SERS effect on cotton brought not only designed functionalization effects. This method turned out to be the useful tool in the identification of the reactive dyes for cotton dyed with low color intensity. In the **Figure 14** there is presented the Raman map on cotton fabric. Spectra presented below map are the reference spectra of cotton and reactive red dye. Red line is the spectrum detected on functionalized cotton surface. In addition to the band characteristic for AgNWs, the signal enhancement and in consequence increase in the intensity of the bands in the region of  $1100\text{--}1600\text{ cm}^{-1}$  is visible. This enhancement concerns main band of cotton at  $1099\text{ cm}^{-1}$  and the bands of reactive dye. When compare this spectrum with the spectrum of cotton modified by AgNWs shown in **Figure 9**, it can be noticed that the cotton and dye

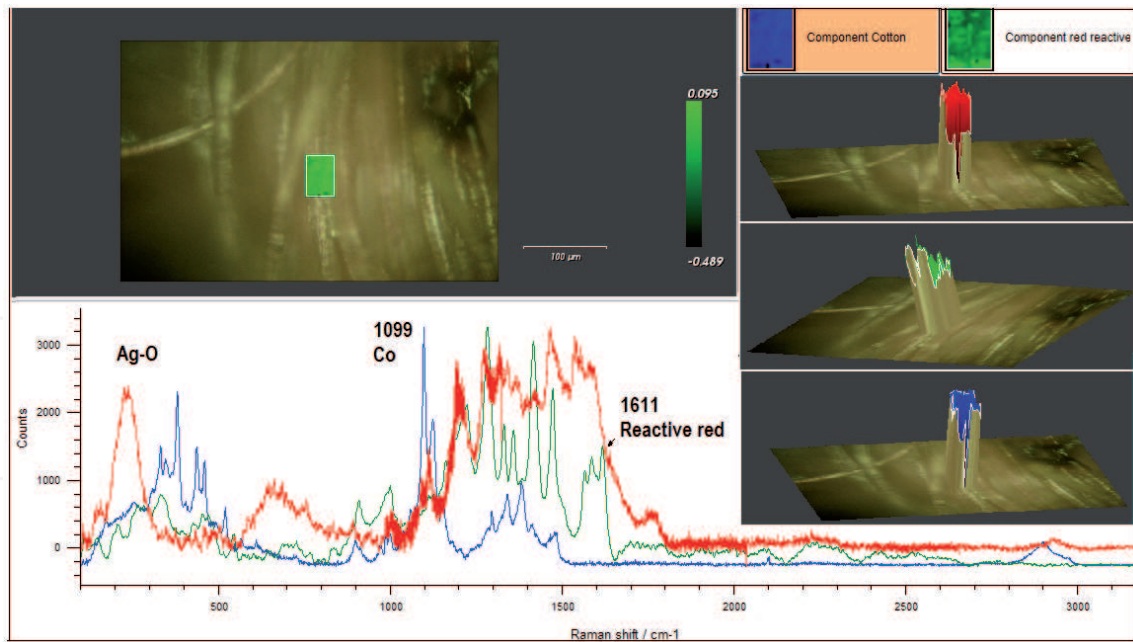


**Figure 14.** Raman map of functionalized cotton fabric. Red line is the measured spectrum, blue line is the reference spectrum of cotton, green line is the reference spectrum of reactive red dye.

bands became visible thanks to this signal enhancement. SERS effect on the cotton surface was accessible only when the thin layer of AgNWs was applied [22].

The SERS effect was also recorded on the wool fibers. The Raman maps of the AgNWs modified wool surface are shown in **Figures 15 and 16**. These maps were done according to a band characteristic of Ag-O coordination and confirm the presence of the AgNWs on the wool. **Figure 16** shows a map of dyed wool and the reference spectra of wool and dye used (reactive red dye) are also presented. Raman maps collected on the wool surface, spectra made point by point, show in some places the enhancement of recorded bands.

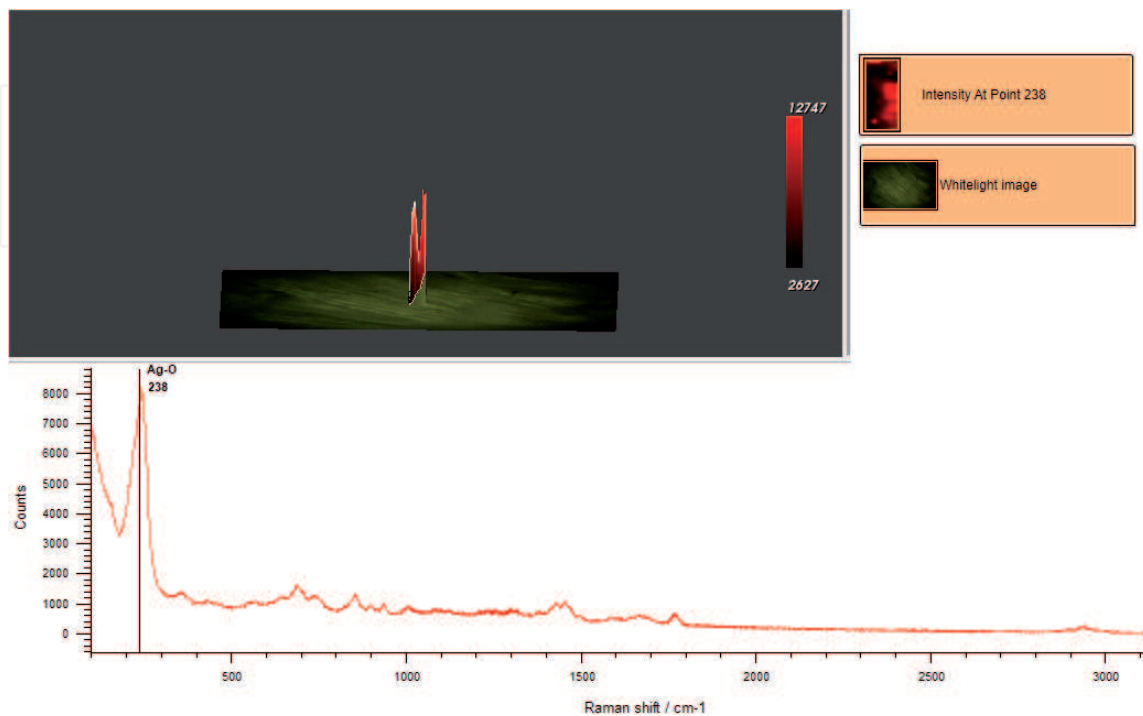


**Figure 15.** Raman 3D map of functionalized wool.

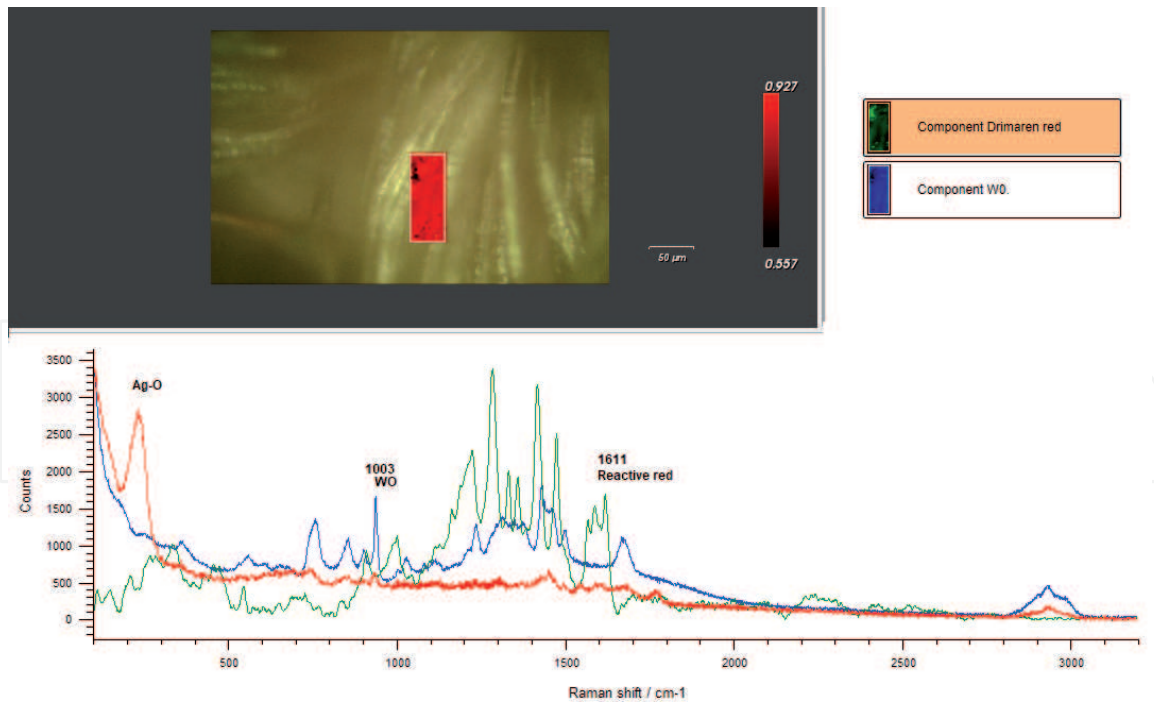


**Figure 16.** Raman map of functionalized dyed wool made. Red line is the measured spectrum, blue line is the reference spectrum of cotton, green line is the reference spectrum of reactive red dye.

In the **Figure 17** there is presented one of such enhanced Raman spectrum. Stars on the **Figure 17** show strengthens bands. As the map is made on the surface of dyed wool, reinforcement of both the wool and the dye strands is observed. However, not all bands are strengthened equally, as at the same time additional SERS bands appear. Additional SERS bands that might be the effect of chemical enhancement of ring vibrations [21, 53]. The SERS effect accompanies the functionalization of

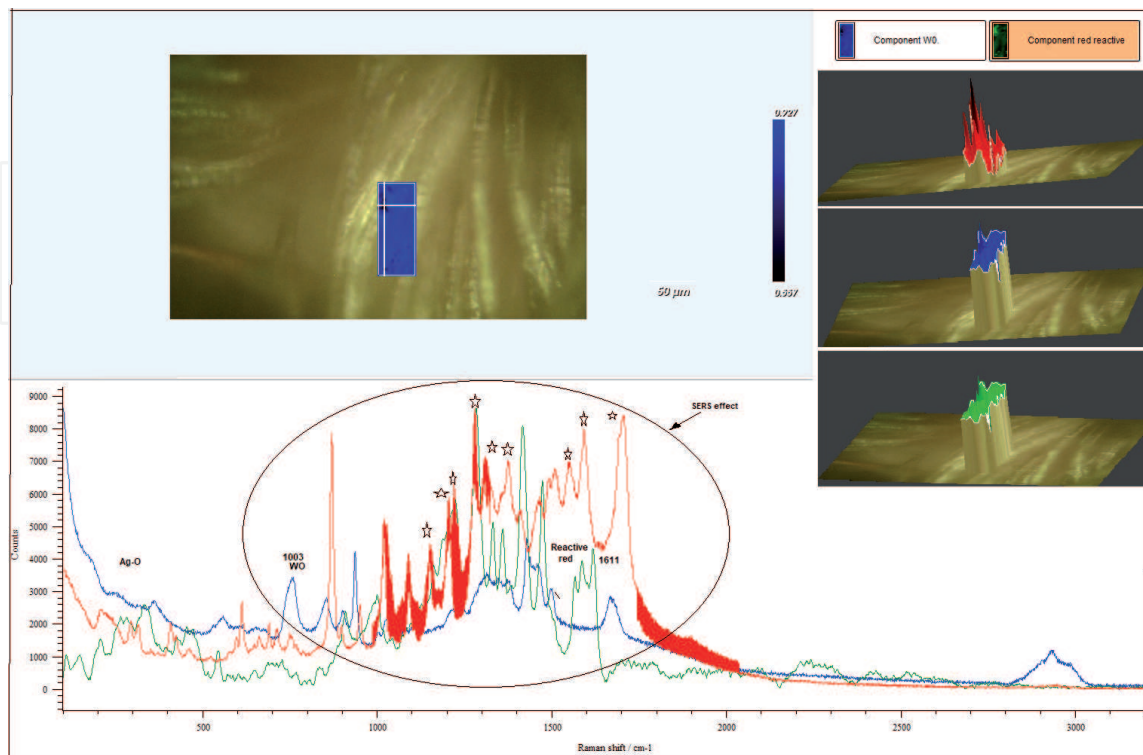


**Figure 17.** Raman map with visible SERS effect of functionalized wool. Red line is the measured spectrum, blue line is the reference spectrum of wool, green line is the reference spectrum of reactive red dye.

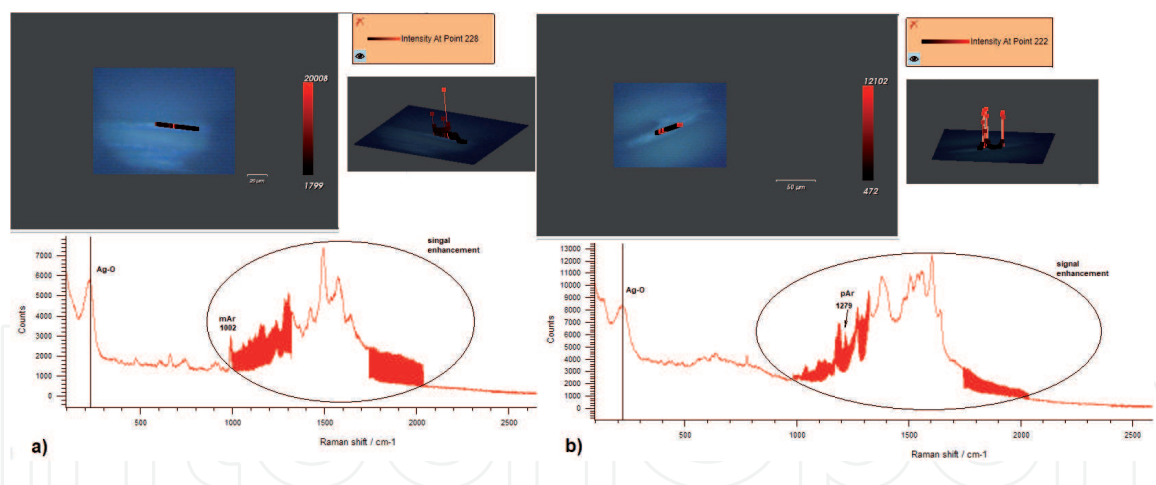


**Figure 18.**  
Raman maps with visible SERS effect on aramid fibers: a) mAr; b) pAr.

fibers with a rough surface and should be studied more deeply as it can be useful in the analysis of textile materials i.e. in the identification of the other elements on the surface.

SERS effect was also identified on aramid fibers, as it is shown in the **Figure 18**.

## 5. Conclusion

Raman spectroscopy is a valuable method in the analysis of textile materials enabling fiber identification and characterization of modification effects. Identification can be carried out for natural and synthetic fiber, both by analyzing their surface and inside the structure. This technique makes also possible to distinguish between the fibers, where IR spectroscopy does not give a definite answer (wool and silk or PA 6 and PA 6.6). Raman spectrum can be also useful in assessment of the textile polymer crystallinity. The Raman spectroscopy special application has found in the study of textile materials functionalized with nanoparticles. They can be analyzed on the surface and inside the fiber. New possibilities are opened by the use of the Raman mapping system which allows the characterization of textile materials with nanoparticles, including SERS analysis. A functionalized textile structure with a noble metal on the surface can be flexible substrates for the surface enhanced Raman spectroscopy (SERS) analysis.

## Acknowledgements

All presented results were carried out on Raman Renishaw InVia Spectrometer purchased the in POIG.01.03.01-00-004/08 Functional nano- and micro textile materials—NANOMITEX project, co-financed by the European Union with the financial resources of the European Regional Development Fund and the National Centre for Research and Development.

The authors would like to thank Ms. Alicja Nejman, Dr. Hubert Schmidt for functionalized fibers used in the research and Ms. Irena Kamińska for the SEM images of fibers.

IntechOpen

IntechOpen

### **Author details**

Dorota Puchowicz\* and Malgorzata Cieslak  
Department of Chemical Textile Technologies, Textile Research Institute,  
LUKASIEWICZ Research Network, Lodz, Poland

\*Address all correspondence to: [dorota.puchowicz@iw.lukasiewicz.gov.pl](mailto:dorota.puchowicz@iw.lukasiewicz.gov.pl)

### **IntechOpen**

---

© 2021 The Author(s). Licensee IntechOpen. This chapter is distributed under the terms of the Creative Commons Attribution License (<http://creativecommons.org/licenses/by/3.0>), which permits unrestricted use, distribution, and reproduction in any medium, provided the original work is properly cited. 

## References

- [1] Hashimoto K., Badarla V.R., Kawai A., Ideguchi T., Complementary vibrational spectroscopy. *Nat Commun* 10, 4411 (2019). DOI:10.1038/s41467-019-12442-9
- [2] Giesz P., Celichowski G., Puchowicz D., Kamińska I., Grobelny J., Batory D., Cieślak M., Microwave-assisted TiO<sub>2</sub>: Anatase formation on cotton and viscose fabric surfaces, *Cellulose* 2016, 23 (3), 2143-2159; DOI:10.1007/s10570-016-0916-z
- [3] Cieślak M., Celichowski G., Giesz P., Nejman A., Puchowicz D., Grobelny J., Formation of nanostructured TiO<sub>2</sub>-anatase films on the basalt fiber surface, *Surface and Coatings Technology*, 2015, 276, 686-695; DOI:10.1016/j.surfcoat.2015.05.045
- [4] Giesz P., Mackiewicz E., Nejman A., Celichowski G., Cieślak M., Investigation on functionalization of cotton and viscose fabrics with AgNWs, *Cellulose* 24 (2017) 409-422. DOI:10.1007/s10570-016-1107-7
- [5] Giesz P., Mackiewicz E., Grobelny J., Celichowski G., Cieślak M., Multifunctional hybrid functionalization of cellulose fabrics with AgNWs and TiO<sub>2</sub>, *Carbohydrate Polymers*, 2017, 177, 397-405, DOI:10.1016/j.carbpol.2017.08.087
- [6] Boufi S., Bouattour S., Ferraria A. M., Vieira Ferreira L.F., Botelho do Rego A.M. Chehimi MM., Vilar M.R., Cotton fibres functionalized with plasmonic nanoparticles to promote the destruction of harmful molecules: An overview *Nanotechnol Rev* 2019; 8:671-680, DOI:10.1515/ntrev-2019-0058
- [7] Syafiuddin A., Toward a comprehensive understanding of textiles functionalized with silver nanoparticles, *J. Chin. Chem. Soc.* 2019;66:793-814., DOI:10.1002/jccs.201800474
- [8] Pakdel E., Daoud W.A., Wang X., Self-cleaning and superhydrophilic wool by TiO<sub>2</sub>/SiO<sub>2</sub> nanocomposite, *Appl. Surf. Sci.*, 2013, 275, 397-402, DOI:10.1016/j.apsusc.2012.10.141
- [9] Radetic M., Functionalization of textile materials with TiO<sub>2</sub> nanoparticles, *J. Photochem. Photobiol. C: 2013*, 16, 62-76, DOI:10.1016/j.jphotochemrev.2013.04.002
- [10] Srinivas K., The role of nanotechnology in modern textiles, *Journal of Chemical and Pharmaceutical Research*, 8 (2016) 173-180.
- [11] Yetisen A.K., Qu H., Manbachi A., Butt H., Dokmeci M.R., Hinstroza J.P., Skorobogatiy M., Khademhosseini A., Hyun Yun S., Nanotechnology in textiles, *ACS Nano*, 10 (2016), 3042-3068, DOI:10.1021/acsnano.5b08176
- [12] Mahmud R., Nabi F., Application of nanotechnology in the field of textile, *Journal of Polymer and Textile Engineering*, 4 (2017), 1-6, <https://www.iosrjournals.org/iosr-jpte/papers/Vol4-Issue1/A04010106.pdf>
- [13] Barani H., Boroumand M. N., Rafiei S., Application of silver nanoparticles as an antibacterial mordant in wool natural, *Fibers and Polymers* 2017, 18, 4, 658-665, DOI:10.1007/s12221-017-6473-8
- [14] Sportelli M. C., Izzi M., Kukushkina E.A., Hossain S. I., Picca R. A., Ditaranto N., Cio N., Can nanotechnology and materials science help the fight against SARS-CoV-2, *Nanomaterials*, 2020, 10, 802; DOI:10.3390/nano10040802
- [15] Arvizo R.R., Bhattacharyya S., Kudgus R., Giri K., Bhattacharya R.,

- Mukherjee P., Intrinsic therapeutic applications of noble metal nanoparticles: Past, present and future, *Chem. Soc. Rev.* 41 (7) (2012) 2943-2970, DOI:10.1039/C2CS15355F.
- [16] Mather R.R., Wardman R.H. (2011), *The chemistry of textile fibres*, RSC publishing, Cambridge 2011.
- [17] Morton W.E., Hearle J.W.S. (1975), *Practical properties of textile fibres*, the textile institute Heinemann, London 1975.
- [18] Pastore C.M., Kiekens P. (2001), *Surface characteristics of Fibers and textiles*, Marcel Dekker Inc., New York 2001.
- [19] Cieslak M., Schmidt H., Swiercz R., Wasowicz W., *Fibers susceptibility to contamination by environmental tobacco smoke markers*, *Text., Res., J.*, 2014, 84(8), 840-853, DOI:10.1177/0040517513509850
- [20] Cieslak M, Puchowicz D, Schmidt H, Evaluation of the possibility of using surface free energy study to design protective fabrics, *Text Res. Journal* 82 (11), 1177-1189, DOI:10.1177/0040517511426612
- [21] Fateixa S., Wilhelm M., Nogueira H. I. S., Trindade T., SERS and Raman imaging as a new tool to monitor dyeing on textile fibres, *Journal of Raman Spectroscopy*, *J. Raman Spectroscopy*, 2016, 47, 1239-1246, DOI:10.1002/jrs.494.
- [22] Puchowicz D., Giesz P., Kozanecki M., Cieślak M., Surface-enhanced Raman spectroscopy (SERS) in cotton fabrics analysis, *Talanta* 2019, 195, 516-524, DOI:10.1016/j.talanta.2018.11.059
- [23] Liu A., Zhang S., Guang S., Ge F., Wang J., Ag-coated nylon fabrics as flexible substrates for surface-enhanced Raman scattering swabbing applications. *Journal of Materials Research*, 35, 1271-1278 (2020). DOI:10.1557/jmr.2020.103
- [24] Kudelski A., Analytical applications of Raman spectroscopy, *Talanta* 76 (2008), 1-8, DOI:10.1016/j.talanta.2008.02.042
- [25] Smith E., Dent G., *Modern Raman Spectroscopy – A Practical approach, applications*, pp, 135-180, John Wiley And Sons, New York, Chichester 2005.
- [26] [https://store.textileexchange.org/wp-content/uploads/woocommerce\\_uploads/2019/11/Textile-Exchange\\_PREFERRED-Fiber-Material-Market-Report\\_2019.pdf](https://store.textileexchange.org/wp-content/uploads/woocommerce_uploads/2019/11/Textile-Exchange_PREFERRED-Fiber-Material-Market-Report_2019.pdf)
- [27] Mather R.R., Wardman R.H. (2011), *Cellulosic fibres [in:] the chemistry of textile fibres*, pp. 22-60 RSC publishing, Cambridge 2011.
- [28] Kavkler K., Demsar A., Examination of cellulose textile fibres in historical objects by micro-Raman spectroscopy, *Spectrochim. Acta Part A* 78 (2011) 740-746, DOI:10.1016/j.saa.2010.12.006.
- [29] Was-Gubala J., Machnowski W., Application of Raman Spectroscopy for differentiation among cotton and viscose Fibers dyed with several dye classes, *Spectroscopy Letters*, 2014, 47:7, 527-535, DOI:10.1080/00387010.2013.820760
- [30] Mather R.R., Wardman R.H. (2011), *Protein fibres [in:] the chemistry of textile fibres*, pp. 61-99, RSC publishing, Cambridge 2011.
- [31] Li-Ling C., Identification of textile fiber by Raman microspectroscopy, *J. Forensic Sci.*, 6 (2007), 55-62.
- [32] Fleming G. D., Finnerty J. J., Campos-Vallette M., C'elis F., Aliaga a. E., Fredes C., Koch R., experimental and theoretical Raman and surface-enhanced Raman scattering study of

- cysteine, *J. Raman Spectrosc.* 2009, 40, 632-638, DOI:10.1002/jrs.2175
- [33] Edwards H. G. M., Farwell D. W., Raman spectroscopic studies of silk, *J. Raman Spectrosc.* 26, 901-909 (1995)
- [34] Nejman A., Kamińska I., Jasińska I., Celichowski G., Cieślak M., Influence of low-pressure RF plasma treatment on aramid yarns properties, *Molecules*, 2020, 25, 3476-3499, DOI:10.3390/molecules25153476
- [35] Stuart B.H., Polymer crystallinity studied using Raman spectroscopy, *Vibrational Spectroscopy* 10 (1996) 79-87
- [36] Boerio E. J, Bahl S.K., Mc Graf G.E., Vibrational analysis of Polyethylenie terephthalate and its Deuterated derivatives, *J. Polym. Sci.*, 1976, 14, 1029-1046.
- [37] Rebollar E., Perez S., Hernandez, M., Domingo C. Martin M., a Ezquerro T.A. Garcia-Ruiz J.P., Castillejo M., Physicochemical modifications accompanying UV laser induced surface structures on poly(ethyleneterephthalate) and their effect on adhesion of mesenchymal cells, *Phys. Chem. Chem. Phys.*, 2014, 16, 17551, DOI:10.1039/c4cp02434f
- [38] Poppe, W. A Kreklau F. H, Bergter R., Process for the identification of the pile of textile materials, in particular for the identification of PA 6 and PA 66 in carpets, DE10011254A1 Patent, 2000.
- [39] Miller J. V, Bartick EG. Forensic analysis of single fibers by Raman spectroscopy. *Appl Spectrosc* 2001;55(12):1729-1732.
- [40] Sagitova E.A., Donfack P., Nikolaeva G. Yu, Prokhorov K.A., Pashinin P.P., Nedorezova P.M., Klyamkina A.N., Materny A., New insights into the structure of polypropylene polymorphs and propylene copolymers probed by low-frequency Raman spectroscopy, *Journal of Physics: Conf. Series* 826 (2017) 012006 DOI:10.1088/1742-6596/826/1/012006.
- [41] Andreassen E. (1999) Infrared and Raman spectroscopy of polypropylene. In: Karger-Kocsis J. (eds) *Polypropylene.*, Pp. 320-328 *Polymer Science and Technology Series*, vol 2. Springer, Dordrecht. DOI:10.1007/978-94-011-4421-6\_46
- [42] Nielsen AS, Batchelder DA, Pyrz R. Estimation of crystallinity of isotactic polypropylene using Raman spectroscopy. *Polymer* 2002; 43: 2671-2676.
- [43] Grieve M. C., Another look at the classification of acrylic fibers, using FTIR microscopy *Science and Justice* 35, 1995, 179-190.
- [44] Sun Y., Gates B., Mayers B., Xia Y., Crystalline silver nanowires by soft solution processing, *Nano Letters*, 16 (2002) 5-168, DOI:10.1021/nl010093y
- [45] Edwards H.G.M., Hakiki S., Raman spectroscopic studies of Nomex and Kevlar fibres under stress, *British Polym. J.* 1989, 21, 505-512.
- [46] Sun Y., Xia Y., Large-scale synthesis of uniform silver nanowires through a soft, self-seeding, polyol process, *Advanced Materials*, 14 (2002) 833-837, DOI:10.1002/1521-4095(20020605)14:11<833::AID-ADMA833>3.0.CO;2-K
- [47] Nghia N.V., Truong N.N.K., Thong N.M., Hung N.P., Synthesis of nanowire-shaped silver by polyol process of sodium chloride, *International Journal of Materials and Chemistry*, 2 (2012) 75-78, DOI:10.5923/j.ijmc.20120202.06
- [48] Wang C.B., Deo G., Wachs I.E., Interaction of polycrystalline silver with oxygen, water, carbon dioxide, ethylene

and methanol: in situ Raman and catalytic studies, *J. Phys. Chem. B* 103 (1999) 5645-5656, DOI:10.1021/jp984363l.

[49] Rashid M.M., Simoncic B., Tomsic B., Recent advances in TiO<sub>2</sub>-functionalized textile surfaces, *Surfaces and Interfaces* 22, 2021, 100890, DOI:10.1016/j.surfin.2020.100890

[50] Cieślak M., Schmidt H., Świercz R., Wąsowicz W., „TiO<sub>2</sub>/Ag modified carpet fibres for the reduction of nicotine exposure”, *FIBRES and TEXTILES in Eastern Europe*, 17, 2 (73), 59-65, 2009.

[51] Cieślak M., Puchowicz D., Kamińska I., SEM/EDS and Raman Micro-Spectroscopy Examination of Titanium-Modified Polypropylene Fibres., *FIBRES and TEXTILES in Eastern Europe* 2014; 22, 3(105): 47-53.

[52] Scepanovic M. J, Gruic-Brojin M., Dohcevic-Mitrovic Z.D. Characterization of anatase TiO<sub>2</sub> nanopowder by variable-temperature Raman spectroscopy. *Sci. Sinter.* 2009; 41: 67-73.

[53] Dong X, Gu H., Kang J., Yuan X., Wu J., Comparative study of surface-enhanced Raman scattering activities of three kinds of silver colloids when adding anions as aggregating agents, *Colloids and Surfaces A: Physicochem. Eng. Aspects*, 368 (2010), 142-147. DOI:10.1016/j.colsurfa.2010.07.029